PHYSICAL REVIEW B **83**, 035203 (2011)

Evidence of localized boron impurity states in (B,Ga,In)As in magnetotransport experiments under hydrostatic pressure

J. Teubert,[1,*] P. J. Klar,[1] A. Lindsay,[2] and E. P. O'Reilly[2,3]

[1]*Institute of Experimental Physics I, Justus Liebig University Giessen, Heinrich-Buff-Ring 16, D-35392 Giessen, Germany*

[2]*Tyndall National Institute, Lee Maltings, Cork, Ireland*

[3]*Department of Physics, University College Cork, Cork, Ireland*

(Received 17 September 2010; published 13 January 2011)

We investigate the magnetotransport properties of n-type (B,Ga,In)As alloys and an n-type GaAs reference sample under hydrostatic pressure up to 16 kbar in the temperature range from 1.6 to 300 K. The free carrier concentration and the mobility of the reference sample are almost independent of the applied hydrostatic pressure. In contrast, the free carrier concentration and the mobility in $B_{0.027}Ga_{0.913}In_{0.06}As$ alloys drop by orders of magnitude over the accessible pressure range. The observations can be explained by assuming that a boron-related density of localized states exists in the vicinity of the conduction band edge of the alloy. The analysis of the pressure-induced changes of the free carrier concentration yields an image of the boron-related density of localized states with characteristic features that are found to be in good agreement with theoretical calculations using a linear combination of isolated states model. Our results provide strong evidence that boron-related states act as isovalent traps in (B,Ga,In)As alloys.

DOI: 10.1103/PhysRevB.83.035203 PACS number(s): 72.20.−i, 71.23.−k, 71.55.Eq, 62.50.−p

I. INTRODUCTION

The properties and electronic structure of many conventional semiconductor alloy systems such as (Al,Ga)As and (Ga,In)As can be well described using the so-called virtual-crystal approximation (VCA). Within the VCA approach, different atoms on the same sublattice are replaced by virtual atoms whose properties are an average of those of the sublattice species. These amalgamation-type alloys are created by substitution with isovalent impurities that are similar in electronegativity and atomic size compared to the substituted atoms. Thus, the substituting atoms do not represent a strong perturbation and the electronic states are well described in terms of the Bloch states of the original host crystal. For example, the properties (e.g., energy gap, lattice constant, effective mass) of the alloy $Ga_{1-x}In_xAs$ can be described with good accuracy by a linear interpolation at $0 \leqslant x \leqslant 1$, that is, between GaAs and InAs.

In contrast, there exist semiconductor alloys that can be regarded as being extreme in the sense that the VCA totally fails to describe aspects of their electronic structure. The most prominent examples that have been studied extensively are Ga(N,As) and (Ga,In)(N,As).[1] Other examples currently of interest are Ga(As,Bi),[2] Zn(O,S),[3] and Zn(O,Se).[4] The cause of the failure of the VCA in all these cases is the large difference in size and electronegativity between the two species alloyed on the anion sublattice. Therefore, in the doping limit the substituting species is referred to as an isovalent trap.[5,6] It should be noted that all known examples for such non-amalgamation-type III-V and II-VI alloys originate from substitution on the anion sublattice. So far, no isovalent traps have been found by substituting on cation sites.

Boron differs strongly from the gallium and indium atoms it replaces on the cationic sublattice of (Ga,In)As; however, the differences are not as large as those between nitrogen and arsenic on the anionic sublattice. It remains controversial, with conflicting evidence in the literature, whether boron acts as an isovalent impurity, forming a non-amalgamation-type alloy when substituted in (Ga,In)As. The first theoretical papers supported the view that a non-amalgamation-type alloy is formed.[7] Shan *et al.* obtained photoreflectance spectra from $B_xGa_{1-x}As$ of different composition x and studied the hydrostatic pressure dependence of the signals.[8] They found that, to a first approximation, the fundamental band gap is not affected by boron. Szwacki and Boguslawski[9] explained the much weaker influence of localized boron states on extended conduction band states (compared to N in GaAs) as being due to symmetry reasons, which stem from the different substitution sites of B and N. By contrast, Hofmann *et al.*, using far-infrared magneto-optic ellipsometry observed a strong increase in the electron effective mass,[10] which is considerably larger than predicted by VCA. This difference in behavior of the energy gap and of the effective mass was explained by Lindsay and O'Reilly, who performed full tight-binding calculations[11] to study the conduction band structure of (B,Ga)As. They found that isolated B impurities, where a B atom has no B second neighbors, have little impact on the electronic structure near the band edge, in agreement with Ref. 9, but that B pairs, where an As atom has two B neighbors, and also larger B clusters, yield localized states in the vicinity of the conduction band edge of the alloy. Their analysis showed that these localized boron cluster states cause the experimentally observed increase in the electron effective mass in (B,Ga,In)As.

Here, we give further theoretical and experimental evidence that boron pairs and clusters indeed form highly localized states in (B,Ga,In)As and thus that B can be regarded as the first example of an isovalent trap substituted on the cation site of a III-V or II-VI semiconductor.

II. EXPERIMENTAL AND THEORETICAL METHODS

Two n-type $B_{0.027}Ga_{0.913}In_{0.06}As$ epitaxial layers are investigated, both of which are lattice-matched to GaAs and possess free carrier concentrations at 1.6 K and ambient pressure of

 ©2011 American Physical Society

$n = 1.2 \times 10^{17}$ and $n = 7.2 \times 10^{17}$ cm^{-3}, respectively. An n-type GaAs epitaxial layer with a free carrier concentration of about $n = 2 \times 10^{18}$ cm^{-3} served as a reference. All samples were grown on (100) GaAs substrates by metal-organic vapor-phase epitaxy. The magnetotransport measurements under hydrostatic pressure were performed in magnetic fields up to 10 T and hydrostatic pressures up to 15 kbar in the temperature range from 1.6 to 300 K. For this purpose, the samples were loaded into a nonmagnetic CuBe clamp pressure cell that was inserted into a superconducting magnet system such that the magnetic field was applied perpendicular to the sample surface. The measurements were performed in a van der Pauw contact geometry. Kerosene was used as the pressure medium and the pressure was determined using a manganin standard.[12]

The band structure of (B,Ga,In)As was calculated using a linear combination of isolated states (LCIS) model, which has been applied very successfully to analyze the effects of nitrogen localized states in Ga(N,As).[13–17] Within this approach, the interaction of the B states with the host (unperturbed) Γ conduction band minimum is calculated taking the complexities of the local B environment into account. Ultralarge (B,Ga,In)As supercells containing $M \sim$ 8000 boron atoms placed at random on the group III sites of the lattice were used. The number M of boron atoms and the size of the supercell were adjusted to obtain the desired boron fraction of 2.7%. In the first step, full tight-binding calculations using an accurate sp^3s^* tight-binding Hamiltonian[11] revealed that four electronic states associated with an isolated boron atom $\psi_{\mathrm{B},0}$ are resonant with the conduction band of the GaAs host, with one of the states being of A_1 symmetry, and the other three states of T_d symmetry. Furthermore, these states are highly localized, with approximately 50% to 60% of each electronic impurity state on the B site and its four As first neighbors. In the second step, one can associate similar localized wave functions $\psi_{\mathrm{B},i,\alpha}, i = 1,\ldots,M, \alpha = 1,\ldots,4$ with each B atom in the system. The wave functions of the perturbed system can then be well represented by a linear combination of $4M$ isolated boron resonant states, including also their interaction with the GaAs conduction band edge wave function. This is the basis of the LCIS model. The distribution of B cluster state energies is derived by first calculating the strength of the interaction between the $4M$ B states and then diagonalizing the $4M \times 4M$ matrix, linking the $4M$ individual B states $\psi_{\mathrm{B},i,\alpha}$ to obtain $4M$ boron cluster states $\psi_{\mathrm{B},l}$ with energies ϵ_l.

III. RESULTS AND DISCUSSION

A. Magnetotransport measurements

Before discussing the influence of hydrostatic pressure on the transport properties of n-(B,Ga,In)As, it is useful to recall the effect of pressure on n-type GaAs. The influence of hydrostatic pressure on the transport properties of n-GaAs is rather weak. For example, the absolute value of the resistivity of the reference sample hardly changes under pressure, increasing by ∼30%, from 1.4×10^{-4} Ω cm at ambient pressure to 1.8×10^{-4} Ω cm at 14 kbar (1.6 K). The same holds for the magnetoresistivity, which shows the typical parabolic behavior. Applying hydrostatic pressure does not change the overall quadratic behavior at all up to the highest pressure value. The only significant influence of pressure is an increasing aperture (broadening) of these parabolas. Again, these changes are rather small, that is, a decrease of only 10% in relative magnetoresistivity at 10 T.

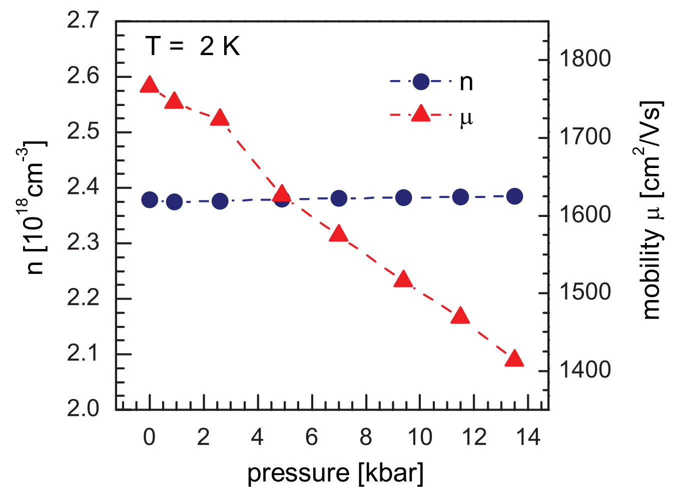

FIG. 1. (Color online) Variation of the free carrier concentration n and mobility μ of an n-type GaAs reference sample as a function of hydrostatic pressure at $T = 2$ K.

The combined analysis of resistivity and Hall data yields a free carrier concentration that is virtually constant under pressure and a mobility that decreases slightly, both depicted in Fig. 1. The broadening of the magnetoresistance parabolas and the decreasing mobility under pressure can be related to the increasing electron effective mass, as reported, for example, in Refs. 18 and 19. In GaAs the fundamental band gap increases under pressure at a rate of 11.5 meV/kbar. The almost-pressure-independent free carrier concentration is a typical feature of n-type doping with hydrogen-like shallow donors. Since the wave function of the shallow donors is delocalized and hybridizes with the states of the conduction band edge, the shallow impurity levels shift under pressure at the same rate as the conduction band edge itself. Thus, the donor activation energy does not change under pressure, and consequently the number of free carriers provided by the donors does not vary with pressure at a constant temperature.

The pressure-induced changes of the transport behavior of n-type (B,Ga,In)As are quite dramatic and very different from those of n-type GaAs, as shown in Fig. 2. Figures 2(b) and 2(d) depict the influence of hydrostatic pressure on the absolute resistivity values for both values of carrier density n. Common to both samples is that hydrostatic pressure induces a strong exponential increase in the absolute resistivity at zero magnetic field. Whereas the effect is quite moderate at room temperature, it is well pronounced at low temperatures, where the increase in resistivity extends over several orders of magnitude and is much stronger than in n-type GaAs. A simple enhancement of the effective mass cannot explain these effects. In the case of the sample with a higher carrier concentration [Figure 2(d)], $\rho_{1.6\,\mathrm{K}}(P)$ seems to increase even more rapidly above 10 kbar. The resistance of the sample with the lower carrier concentration grew too large to allow accurate and reliable measurements above 5.6 kbar.

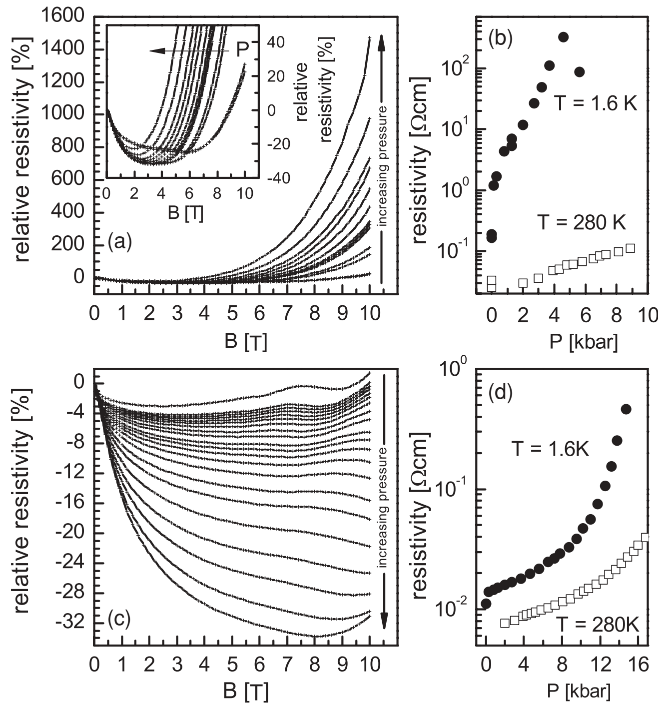

FIG. 2. (a) Relative magnetoresistance at 1.6 K and (b) absolute resistivity at zero magnetic field versus applied pressure at 1.6 and 280 K for a $B_{0.027}Ga_{0.913}In_{0.06}As$ epitaxial layer with $n(P = 0) = 1.2 \times 10^{17}$ cm^{-3}. (c,d) Corresponding graphs for a $B_{0.027}Ga_{0.913}In_{0.06}As$ epitaxial layer with $n(P = 0) = 7.2 \times 10^{17}$ cm^{-3}.

The magnetoresistance behavior under pressure of the two (B,Ga,In)As samples is depicted in Figs. 2(a) and 2(c). In the case of the sample with a lower n [Fig. 2(a)], one observes a dramatic increase in the positive magnetoresistance contribution at high fields that can be attributed to wave function shrinkage in hopping transport.[20] The negative contribution hardly changes (as seen best in the magnification in the inset in Fig. 2(a) and maintains its value of approximately −30%, while the onset of the exponential positive contribution is shifted toward lower magnetic fields, leading to extraordinary high values of more than 1500% at 10 T.

At ambient pressure already, this sample is on the verge of leaving the regime of band transport and entering the hopping conduction regime and a considerable amount of the transport has taken place between localized states; otherwise, wave function shrinkage effects would not be visible. Under pressure these shrinkage effects become even more pronounced, indicating the important role of localized states. This is a strong indication of a shift of the Fermi level toward the region of localized states. In general, the pressure-induced behavior of this sample resembles the temperature-dependent behavior of n-type (B,Ga,In)As “hopping” samples, which is discussed in detail in Ref. 20.

At first sight the results of the metallic sample (higher n) are different. For this sample, Fig. 2(c) shows that applying pressure leads to a strong enhancement of the negative magnetoresistance effects. The minimum of the magnetoresistance curves decreases from −3% at ambient pressure toward approximately −30% at 14 kbar, which is about the same value

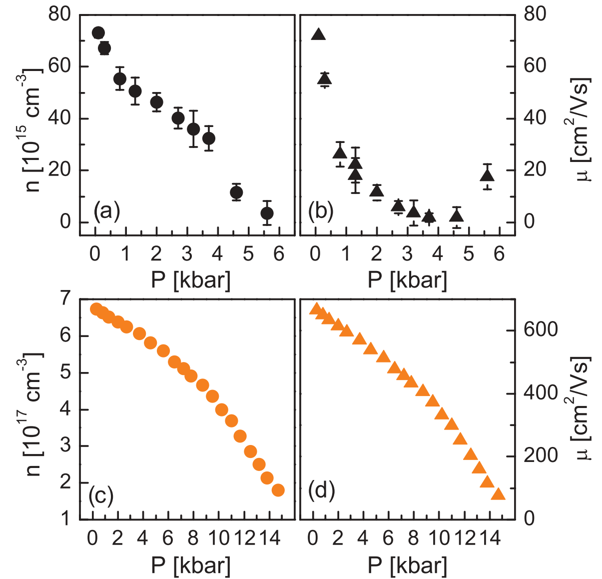

FIG. 3. (Color online) Dependence of free carrier concentration n and electron mobility μ on hydrostatic pressure for the two $B_{0.027}Ga_{0.913}In_{0.06}As$ samples with $n(P = 0) = 1.2 \times 10^{17}$ cm^{-3} (a,b) and $n(P = 0) = 7.2 \times 10^{17}$ cm^{-3} (c,d). Data obtained from combined resistivity and Hall measurements at 1.6 K.

as observed in all samples that show indications of hopping transport. At the highest accessible pressure, the increase in ρ above 8 T may be interpreted as the onset of the wave function shrinkage effect, again indicating a shift in the Fermi level toward a region of localized states. The more pronounced negative magnetoresistance effects under pressure are then easily explained by the increasing disorder due to potential fluctuations within the framework of weak Anderson localization.[21,22]

Figure 3 presents the pressure dependence of the free carrier concentration n and mobility μ for the two n-type (B,Ga,In)As samples determined from the combined Hall and resistivity analysis. Both samples show qualitatively similar results, that is, a strong decrease in both quantities, n and μ, with pressure. In the case of the samples with a lower free carrier concentration, n decreases by almost 2 orders of magnitude, with the rate of decrease rising considerably above 4 kbar. The mobility decreases up to 4 kbar only and then increases slightly again for higher pressures. For the sample with higher n, a monotonic decrease is observed for both n and μ. Above approximately 8 kbar, this occurs at increasing rates. At ambient pressure, both samples show clear band transport with quite high electron mobilities. This allows one to conclude that the Fermi level at $p = 0$ must be close to the extended conduction band states of the host.

B. LCIS defect level calculations

For the discussion of the origin of the experimental findings just described, it is useful to take a closer look at the results of the LCIS calculations. The histogram in Fig. 4 depicts the energy distribution of the boron-related localized cluster states, which stretches out considerably in energy. It should be noted that the extended states of the host crystal are not included in the histogram. The calculations show distinct structure in the density of boron-related states. Clearly visible

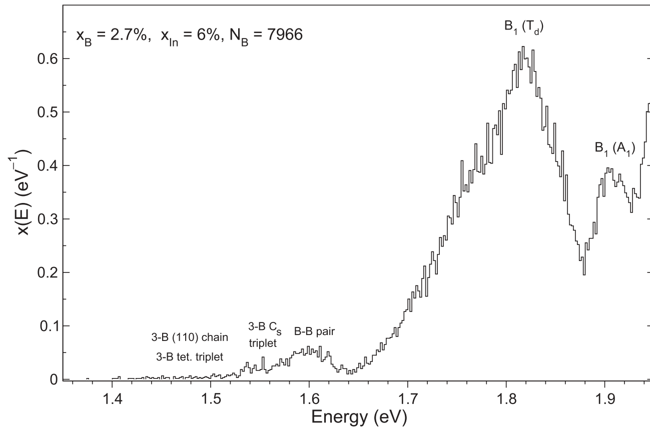

FIG. 4. Density of boron-related states calculated within the LCIS approach, using an ultralarge supercell containing $N_B = 7966$ boron atoms. $x(E)$ gives the fraction of B states with energy E, with $\int_0^\infty x(E)/4\,dE = 0.027$. $T = 0\,K$. Energies are given with respect to the valence band maximum.

are the two peaks related to isolated boron B_1, with T_d and A_1 symmetry, at approximately 1.8 and 1.9 eV, respectively. In addition, there also exist cluster states at lower energies, that is, in the vicinity of the band edge, which is located at $E_C = 1.45$ eV at 10 K. Those states are attributed to boron pair states around 1.6 eV and to higher cluster states such as B-triplet states or longer B chains at lower energy. Their total number is of the order of 10^{18} cm^{-3}, that is, of a magnitude similar to that of the donor concentration of the (B,Ga,In)As samples under study. The structure in the low-energy tail of the histogram cannot be better resolved, reflecting the limitations of supercell size in the calculations. Nevertheless, the calculations show that a broad density of states due to boron cluster states can be anticipated in the vicinity of the conduction band edge of $B_{0.027}Ga_{0.913}In_{0.06}As$. By calculating the histogram of the boron-related states as a function of energy for both 0 and 15 kbar we find that the pressure-induced shifts are negligible. Likewise, we estimate from measurements on undoped samples that the temperature-induced shift of the B states is considerably smaller than that of the conduction band edge. Both these estimated variations are consistent with measurements on other localized states, including N-related states in GaNAs and GaNP.[23–25]

In contrast, it is reasonable to assume that the extended shallow donor states and the band states at the Γ-conduction band edge shift at the same rate to higher energies with either decreasing temperature or increasing pressure. This implies that the density of states associated with localized boron states is then shifted downward with respect to the density of states of the extended states. As a result, the number of localized states below the conduction band edge, which may act as electron traps, increases with decreasing temperature or increasing pressure. The first boron-related states with a significant fraction of the corresponding density of states, which will be approached by the conduction band edge from the low energy side, are the 3-B tetrahedral triplets and 3-B chains. The different situations resulting at 2 K and at room temperature are illustrated schematically in Fig. 5. The following additional parameters were used: $dE_C/dP =$

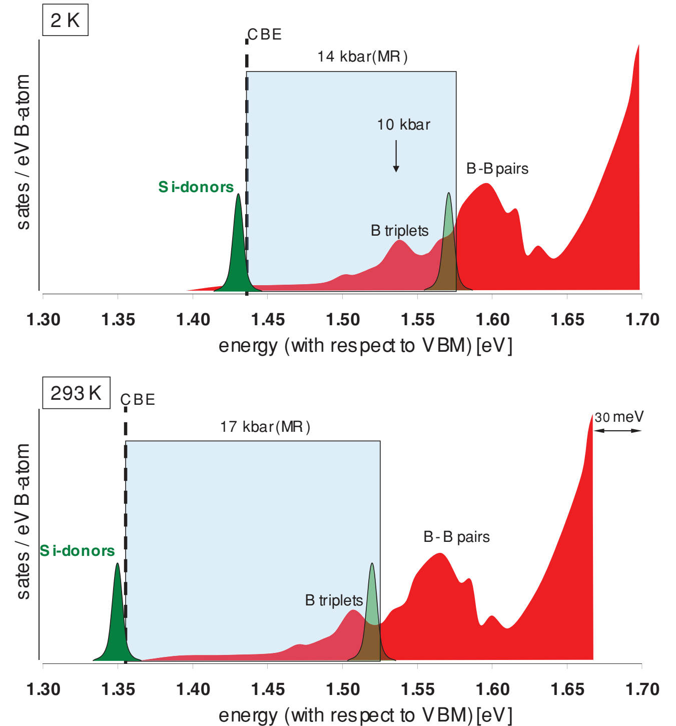

FIG. 5. (Color online) Schematic illustration of the consequences of applying hydrostatic pressure, when the conduction band edge is shifted through the distribution of localized B cluster states. The two plots correspond to low and high temperature. Boron-localized states are shown in red; silicon donor states, in green. Gray areas indicate the pressure range accessible in transport measurements.

10 meV/kbar (determined from PR measurements under pressure using an undoped $B_{0.027}Ga_{0.913}In_{0.06}As$ reference sample), $dE_B/dP = 0$ meV/kbar, $E_C(P = 0\text{ kbar}, T = 10\text{ K}) = 1.45$ eV, and $E_C(P = 0\text{ kbar}, T = 293\text{ K}) = 1.36$ eV, as well as a temperature-induced energy shift of the boron density of states by about 30 meV between 293 and 1.6 K. At low temperatures, a significant portion of the boron cluster states, namely, the several triplet states, that lie above the conduction band edge at ambient pressure is then located below the conduction band edge at 15 kbar in this scenario.

C. Comparison of theory and experiment

With this picture in mind, the reduction of the free carrier concentration n under pressure is closely connected to the boron cluster state distribution. The reduction is due to the trapping of electrons by the localized boron states that drop below the conduction band edge with increasing pressure, that is, the Fermi level shifts toward the region of localized states. In this simplified picture, the donor states serve as a reservoir of carriers that loses electrons into boron states with increasing pressure P. This explanation allows further analysis of the $n(P)$ data. By numerical differentiation one obtains dn/dP, which is a measure of the density of boron states that fall below the conduction band edge. The results of this analysis performed with the $n(P)$ data obtained at 1.6 and 280 K for the $B_{0.027}Ga_{0.913}In_{0.06}As$ with $n = 7.2 \times 10^{17}$ cm^{-3} are presented in Fig. 6. In the case of the sample with the lower n, the error bars for the Hall data were too large, as the

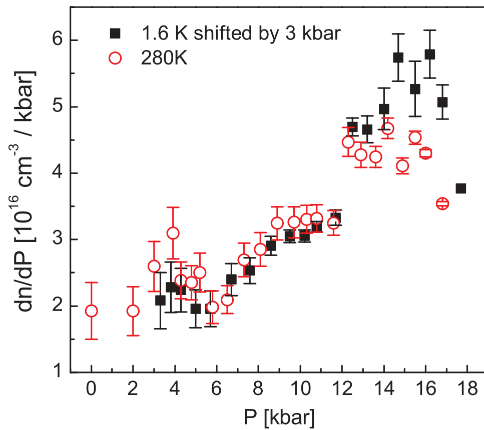

FIG. 6. (Color online) Comparison of dn/dP values obtained at 1.6 K and at room temperature. The 1.6 K data have been shifted by 3 kbar toward higher P to account for the difference in the temperature shifts of the energy levels associated with localized and extended states.

high sample resistance did not allow reliable derivation of the dn/dP data points by numerical differentiation.

Figure 5 suggests that the portion of the density of states of the boron-localized states passed by the conduction band edge under pressure at 2 K is different from that at 293 K due to the larger temperature-induced shift of the conduction band edge compared to that of the boron cluster states. Consequently, the maximum in dn/dP should appear at higher pressure values at room temperature. This is in excellent agreement with experiment, as presented in Fig. 6, which shows the extracted dn/dP data at 280 K [(red) circles]. The (black) squares represent the low-temperature data shifted by 3.0 kbar toward a higher pressure (equivalent to a 30-meV shift in energy). The good agreement match provides further support for the validity of the model shown in Fig. 5. Clear similarities can be seen when the dn/dP data are compared to the theoretical density-of-states calculations. The maximum of dn/dP, at about 15 kbar, can be interpreted as being due to the C_S triplet states. Using $N_{\text{triplet}} \approx 4x^3$, the total number of these states can be estimated as 1×10^{18} cm^{-3} for a boron concentration $x = 0.027$. This is close to the measured free carrier concentration of $n = 7.2 \times 10^{17}$ cm^{-3} at ambient pressure, which can be regarded as the size of the free carrier reservoir. The rough estimate of the number of B states is slightly higher than the available free carrier concentration. A likely explanation is that this is either related to the width of the B triplet density of states or that not all higher B clusters act as efficient electron traps. In either case, the details of the trapping mechanism of the different B clusters needs further study.

Moreover, the considerably decreased mobility observed for both samples under pressure (Fig. 3) is also in concordance with the presence of boron cluster states in the vicinity of the Fermi level. The cluster states close to the Fermi level are efficient scattering centers. With increasing pressure the number of boron states below the conduction band edge increases and the Fermi level is located within a region of localized states and thus typical impurity band mobilities of the order of 10 cm^2 V^{-1} s^{-1} are measured even for the sample with high n, which was originally metallic at ambient pressure.

IV. CONCLUSIONS

The alloy system (B,Ga,In)As possesses a complex electronic structure with manifold interactions between localized and extended states. Despite the difficulties brought about by this complexity, the properties is well explained by the existence of a density of localized boron states that lies in the same energy range as the extended states associated with the conduction band edge of the alloy. These boron cluster states act as efficient electron traps when situated below the Fermi level. The number of boron-related states below the Fermi level can be tuned by applying hydrostatic pressure or by varying the temperature of the sample. The tunability arises because of the differences in pressure-induced and temperature-induced shifts between the boron energy levels, on the one hand, and the energies of the extended conduction band states and donor states, on the other hand. As a consequence, magnetotransport experiments under pressure on n-type (B,Ga,In)As alloys yield entirely different results than in corresponding studies on n-type GaAs. A pressure-induced metal-insulator transition occurs in the n-type alloy due to the trapping of electrons in localized B-related cluster states that shift below the band gap under pressure or at low temperature. The derivative of the free carrier concentration with respect to the applied pressure reflects the density of states of the localized boron clusters. The results of the experiments are in full agreement with theoretical calculations of the boron-related density of states performed in the framework of the LCIS model, yielding a conclusive picture of the electronic band structure of the (B,Ga,In)As alloy. In fact, it can be concluded that boron atoms and clusters show the characteristic behavior of isovalent electron traps, rendering boron as the first known isovalent trap induced by cationic substitution.

ACKNOWLEDGMENT

We would like to thank V. Gottschalch (U. Leipzig) for the provision of samples used in the context of this work.

[*]Corresponding author. joerg.teubert@exp1.physik.uni-giessen.de

[1]W. Shan, W. Walukiewicz, J. W. Ager III, E. E. Haller, J. F. Geisz, D. J. Friedman, J. M. Olson, and S. R. Kurtz, Phys. Rev. Lett. **82**, 1221 (1999).

[2]K. Alberi, O. D. Dubon, W. Walukiewicz, K. M. Yu, K. Bertulis, and A. Krotkus, Appl. Phys. Lett. **91**, 051909 (2007).

[3]B. K. Meyer, A. Polity, B. Farangis, Y. He, D. Hasselkamp, Th. Krömer, and C. Wang, Appl. Phys. Lett. **85**, 4929 (2004).

[4]M. A. Mayer, D. T. Speaks, K. M. Yu, S. S. Mao, E. E. Haller, and W. Walukiewicz, Appl. Phys. Lett. **97**, 022104 (2010).

[5]W. Czaja, Festkoerperprobleme **11**, 65 (1971).

[6]J. J. Hopfield, D. G. Thomas, and R. T. Lynch, Phys. Rev. Lett. **17**, 312 (1966).
[7]G. L. W. Hart and A. Zunger, Phys. Rev. B **62**, 13522 (2000).
[8]W. Shan, W. Walukiewicz, J. Wu, K. M. Yu, J. W. Ager, S. X. Li, E. E. Haller, J. F. Geisz, D. J. Friedman, and S. R. Kurtz, J. Appl. Phys. **93**, 2696 (2003).
[9]N. Gonzalez Szwacki and P. Boguslawski, Phys. Rev. B **64**, 161201 (2001).
[10]T. Hofmann, M. Schubert, G. Leibiger, and V. Gottschalch, Appl. Phys. Lett. **90**, 182110 (2007).
[11]A. Lindsay and E. P. O'Reilly, Phys. Rev. B **76**, 075210 (2007).
[12]O. E. Andersson and B. Sundqvist, Rev. Sci. Instrum. **68**, 1344 (1997).
[13]A. Lindsay and E. P. O'Reilly, Solid State Commun. **118**, 313 (2001).
[14]A. Lindsay and E. P. O'Reilly, Phys. Rev. Lett. **93**, 196402 (2004).
[15]A. Lindsay and E. P. O'Reilly, Physica E **21**, 901 (2004).
[16]F. Masia, G. Pettinari, A. Polimeni, M. Felici, A. Miriametro, M. Capizzi, A. Lindsay, S. B. Healy, E. P. O'Reilly, A. Cristofoli, G. Bais, M. Piccin, S. Rubini, F. Martelli, A. Franciosi, P. J. Klar, K. Volz, and W. Stolz, Phys. Rev. B **73**, 073201 (2006).
[17]G. Pettinari, F. Masia, A. Polimeni, M. Felici, A. Frova, M. Capizzi, A. Lindsay, E. P. O'Reilly, P. J. Klar, W. Stolz, G. Bais, M. Piccin, S. Rubini, F. Martelli, and A. Franciosi, Phys. Rev. B **74**, 245202 (2006).
[18]D. Lancefield, A. R. Adams, and M. A. Fisher, J. Appl. Phys. **62**, 2342 (1987).
[19]D. Lancefield, A. R. Adams, and B. J. Gunney, Appl. Phys. Lett. **45**, 1121 (1984).
[20]J. Teubert, P. J. Klar, and W. Heimbrodt, Phys. Stat. Sol. C **5**, 858 (2008).
[21]J. Teubert, P. J. Klar, W. Heimbrodt, V. Gottschalch, A. Lindsay, and E. P. O'Reilly, Phys. Status Solidi B **244**, 431 (2007).
[22]J. Teubert, P. J. Klar, W. Heimbrodt, K. Volz, W. Stolz, and P. Thomas, Appl. Phys. Lett. **84**, 747 (2004).
[23]P. J. Klar, H. Grüning, W. Heimbrodt, J. Koch, F. Höhnsdorf, W. Stolz, P. M. A. Vicente, and J. Camassel, Appl. Phys. Lett. **76**, 3439 (2000).
[24]X. Liu, M.-E. Pistol, L. Samuelson, S. Schwetlick, and W. Seifert, Appl. Phys. Lett. **56**, 1451 (1990).
[25]M. Felici, A. Polimeni, A. Miriametro, M. Capizzi, H. P. Xin, and C. W. Tu, Phys. Rev. B **71**, 045209 (2005).